Optimum Placement of UAV as Relays

Yunfei Chen, *Senior Member, IEEE,* Wei Feng, Gan Zheng, *Senior Member, IEEE*

Abstract— Unmanned aerial vehicles (UAVs) as aerial base stations or relays are becoming increasingly important in communications. In this letter, the optimum placement of a relaying UAV for maximum reliability is studied. The total power loss, the overall outage and the overall bit error rate are derived as reliability measures. The optimum altitude is investigated for both static and mobile UAVs. Numerical results show that different reliability measures have slightly different optimum altitudes and that decode-and-forward is better than amplify-and-forward.

Index Terms— Bit error rate, outage, placement, power loss, unmanned aerial vehicles.

I. INTRODUCTION

Unmanned aerial vehicles (UAVs) are becoming more and more attractive as aerial base stations or relays to provide network coverage [1], [2]. One challenge in UAV communications is the flight time constraint of UAV [3]. Another important issue is the placement of the UAV [4].

Several researchers have worked on the optimum placement of UAVs as aerial base stations. In the seminal paper [5], the authors proposed a path loss model that accommodates both LOS and NLOS conditions. In [6], the authors extended the result to a 3D space. In [7], the authors considered the optimum placement of UAV in device-to-device communications. References [8] - [11] further explored the use of multiple UAVs to cover a certain area. All these works have provided very useful insights on the placement of UAV as an aerial base station. However, an important issue that has been largely ignored in these works is that UAV may have limited storage and processing capabilities so that the data it receives from the ground user will have to be relayed to a remote ground station for further processing.

Works on the optimum placement of UAVs as relays have also been conducted. For example, reference [12] proposed a variable-rate approach to optimize the achievable rate for a relaying UAV. Reference [13] studied the placement of a relaying UAV in a multi-rate network. Similarly, in [14], the flying path of the UAV was optimized. These works have mainly focused on the relaying distance of UAV, not the altitude. Also, they did not consider the fact that the ground user may be more power-limited than the remote station such that the power loss in the hop from the ground user to UAV needs to be minimized.

In this work, we study the optimum altitude of the UAV as a relaying station using realistic UAV channel models

Yunfei Chen is with the School of Engineering, University of Warwick, Coventry, UK, CV4 7AL. e-mail: Yunfei.Chen@warwick.ac.uk

Wei Feng is with the Department of Electronic Engineering, Tsinghua University, Beijing 100084, China. He is the corresponding author. e-mail: fengwei@tsinghua.edu.cn

Gan Zheng is with the School of Electronic and Electrical and Systems Engineering, Loughborough University, Loughborough, UK LE11 3TU. e-mail: g.zheng@lboro.ac.uk.
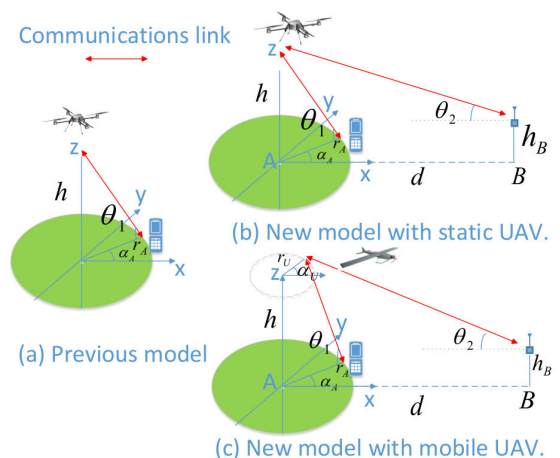

Fig. 1. Diagrams of the considered systems.

and numerical search by focusing on the reliability metrics in terms of power loss, outage probability and bit error rate (BER). Both static and mobile UAVs are considered. Numerical results show that the altitude that optimizes the relaying performance is significantly different from the altitude that optimizes the hop from the ground user to UAV. They also show that different performance measures have slightly different optimum altitudes and that decode-and-forward (DF) performs better than amplify-and-forward (AF).

Compared with [5] - [11], this work considers both hops from the ground user to UAV and from UAV to the remote station in the placement optimization, while [5] - [11] only considered the hop from the ground user to UAV. Also, compared with [12] - [14], this work uses realistic UAV channel models and fixes the UAV on top of the ground user to minimize the power loss for the ground user, while [12] - [14] used standard wireless channel models and the UAV was placed between the ground user and the remote station. Moreover, this work focuses on the reliability, while the previous works focused on the capacity.

II. SYSTEM MODEL

Consider a UAV communications system as shown in Fig. 1. The ground user is located in a circle with radius r_A and angle α_A in polar coordinates. If the UAV is static, it is fixed on top of the center of the circle with an altitude of h, as shown in Fig. 1(b). If the UAV is mobile, it flies in a circle with radius r_U and angle α_U at some time, as shown in Fig. 1(c). The remote station is located d meters away from the center of the coverage area with a height of h_B. The ground user, the UAV and the remote station form a three-node relaying system, where the ground user acts as the source or destination node

and the remote station acts as the destination or source node, respectively, depending on the direction of communications, while the UAV acts as relay in both directions.

The UAV can be some heavy-duty drone with enough payload to carry the wireless equipment. For example, the DJI Agras MG-1 drone can carry a payload of up to 10 kg, while small cell modules Cisco USC 8718/8818 weigh less than 1 kg and Nokia mini 4G base station weighs between 2 and 5 kg. The payload and flight control of drones can affect the system design in some applications or terrains. For the static UAV case, rotary-wing drones can be used, while for the mobile UAV case, fixed-wing drones can be used. Also, the UAV is expected to provide coverage for users within the circle in Fig. 1. A network of UAVs could be used to provide better coverage. However, coordination, such as collision avoidance and interference management, may outweigh the benefits of better performance. For simplicity, it is not considered here.

Compared with the model in [5] - [11] given by Fig. 1(a), where the UAV acts as an aerial base station, our new models account for the hop from the UAV to the remote station. Also, compared with [12] - [14], the UAV in our work stays on top of the center of the circle or circles around this area to minimize the power loss for the ground user, while the UAV in [12] - [14] flies or stays between the ground user and the remote station. The ground user may be battery-powered with low transmission power, so it is necessary for the UAV to stay on top of it to minimize the power loss, as the relaying performance is determined by the weaker hop. For multiple users, we assume that the cell radius is r_A so that the obtained result is the worst-case scenario to guarantee a minimum performance at the edge of the cell, similar to [5] - [11]. Users inside the cell are expected to have better performances. In the case of multiple users, orthogonal channels can be used to avoid co-channel interference.

From Fig. 1, one has the coordinates for the ground user as $(r_A \cos(\alpha_A), r_A \sin(\alpha_A), 0)$ and the coordinates for the remote ground station as $(d, 0, h_B)$. For static UAV in Fig. 1(b), the coordinates for the UAV is $(0, 0, h)$. For the mobile UAV in Fig. 1(c), the coordinates for the UAV is $(r_U \cos(\alpha_U), r_U \sin(\alpha_U), h)$. The time variance has been included in α_U. Using these coordinates, for static UAV, the distance between the ground user and the UAV is

$$d_1 = \sqrt{r_A^2 + h^2}, \qquad (1)$$

and the distance between the UAV and the remote station is

$$d_2 = \sqrt{(h - h_B)^2 + d^2}. \qquad (2)$$

For mobile UAV, the distance between the ground user and the UAV is

$$d_1 = \sqrt{h^2 + r_U^2 + r_A^2 - 2r_A r_U \cos(\alpha_U - \alpha_A)}, \qquad (3)$$

and the distance between the UAV and the remote station is

$$d_2 = \sqrt{(h - h_B)^2 + r_U^2 + d^2 - 2dr_U \cos(\alpha_U)}, \qquad (4)$$

where α_U is the angle between the UAV and the x axis denoted in Fig. 1(c). It is determined by $\alpha_U = \omega t + \alpha_0$, where ω is the angular velocity of the UAV and α_0 is the initial angle. Using

these distances, the path loss in the hop from the ground user to the UAV is given by [5]

$$PL^A = \frac{A_1}{1 + a_1 e^{-b_1(\theta_1 - a_1)}} + B_1, \qquad (5)$$

where $A_1 = \eta_{LOS1} - \eta_{NLOS1}$, $B_1 = 20\log_{10}(d_1) + 20\log_{10}(4\pi f/c) + \eta_{NLOS1}$, f is the carrier frequency, c is the speed of light, η_{LOS1}, η_{NLOS1}, a_1 and b_1 are constants related to the propagation environments in this link, and $\theta_1 = \frac{180}{\pi}\arctan(\frac{h}{r_A})$. The path loss in the hop from the UAV to the remote station follows the same model as

$$PL^B = \frac{A_2}{1 + a_2 e^{-b_2(\theta_2 - a_2)}} + B_2, \qquad (6)$$

where $A_2 = \eta_{LOS2} - \eta_{NLOS2}$, $B_2 = 20\log_{10}(d_2) + 20\log_{10}(4\pi f/c) + \eta_{NLOS2}$, η_{LOS2}, η_{NLOS2}, a_1 and b_1 are constants related to the propagation environments in the this link, and $\theta_2 = \frac{180}{\pi}\arctan(\frac{h - h_B}{d})$. In [5] - [11], only PL^A was considered in the optimization of h. Next, we will derive the overall outage probability and overall BER in a separate section to improve presentation.

III. OUTAGE AND BER ANALYSIS

The absolute power loss is given by

$$Q_A = 10^{\frac{PL^A}{10}},$$
$$Q_B = 10^{\frac{PL^B}{10}}. \qquad (7)$$

If AF is used, the UAV receives the information from the ground user and forwards it to the remote station without any further processing or the other way around if the remote station transmits data. Then, the end-to-end signal-to-noise ratio (SNR) can be shown as

$$\gamma_{AF} = \frac{\gamma_A + \gamma_B}{\gamma_A + \gamma_B + 1}, \qquad (8)$$

where $\gamma_A = \frac{|g_A|^2}{2\sigma^2 Q_A}$ and $\gamma_B = \frac{|g_B|^2}{2\sigma^2 Q_B}$ are the hop SNRs, g_A and g_B are the fading coefficients, and $2\sigma^2$ is the noise variance at both the ground user and the remote station. Assume Nakagami-m fading channels so that one has

$$f_{|g_A|}(x) = \frac{2}{\Gamma(m_A)}\left(\frac{m_A}{\Omega_A}\right)^{m_A} x^{2m_A - 1} e^{-\frac{m_A x^2}{\Omega_A}},$$
$$f_{|g_B|}(x) = \frac{2}{\Gamma(m_B)}\left(\frac{m_B}{\Omega_B}\right)^{m_B} x^{2m_B - 1} e^{-\frac{m_B x^2}{\Omega_B}}, \qquad (9)$$

where $\Gamma(\cdot)$ is the Gamma function [15, eq. (8.310.1)], m_A and m_B are the Nakagami m parameters and $\Omega_A = E\{|g_A|^2\}$ and $\Omega_B = E\{|g_B|^2\}$ are the average fading powers.

Using (8) and (9), the cumulative distribution function (CDF) of γ_{AF} can be derived as [16]

$$F_{AF}(x) = 1 - 2e^{-(\frac{1}{\beta_1} + \frac{1}{\beta_2})x} \sum_{n=0}^{\alpha_1 - 1} \sum_{k=0}^{\alpha_2 - 1} \sum_{m=0}^{k} C_1(n, k, m)$$

$$K_{n-m+1}(2\sqrt{\frac{x(x+1)}{\beta_1 \beta_2}})(\frac{x+1}{x})^{\frac{n+m+1}{2}} x^{\alpha_1 + k}, \qquad (10)$$

where $\alpha_1 = m_A$, $\beta_1 = \frac{\Omega_A}{2\sigma^2 m_A Q_A}$, $\alpha_2 = m_B$, $\beta_2 = \frac{\Omega_B}{2\sigma^2 m_B Q_B}$, $C_1(n, k, m) = \frac{\beta_1^{\frac{n-m+1-2\alpha_1}{2}} \beta_2^{\frac{m-n-1-2k}{2}}}{m!(k-m)!n!(\alpha_1 - n - 1)!}$, and $K_{n-m+1}(\cdot)$ is

the $(n - m + 1)$-th modified Bessel function of the second type [15, eq. (8.432.1)]. Using (10), the outage probability can be derived as

$$P_o^{AF} = Pr\{\gamma_{AF} < \gamma_{th}\} = F_{AF}(\gamma_{th}). \qquad (11)$$

The exact bit error rate (BER) could be calculated by using the exact end-to-end SNR in (8), but this does not lead to a simple expression for optimization [17]. Thus, an approximate BER can be calculated by approximating the exact end-to-end SNR in (8) with the harmonic mean as $\gamma_{AF} \approx \frac{\gamma_A \gamma_B}{\gamma_A + \gamma_B}$ and using the harmonic mean for binary phase shift keying (BPSK) as

$$
P_e^{AF} \approx \frac{1}{2} - \sum_{n=0}^{\alpha_1-1} \sum_{k=0}^{\alpha_2-1} \sum_{m=0}^{k} C_1(n,k,m)(\frac{4}{\sqrt{\beta_1\beta_2}})^{n-m+1}
$$
$$
\frac{\Gamma(\alpha_1 + k + n - m + 1.5)\Gamma(\alpha_1 + k - n + m - 1.5)}{\Gamma(\alpha_1 + k + 1)((\frac{1}{\sqrt{\beta_1}} + \frac{1}{\sqrt{\beta_2}})^2 + 1)^{\alpha_1+k+n-m+1.5}}
$$
$$
F(\alpha_1 + k + n - m + 1.5, n - m + 1.5; \alpha_1 + k + 1;
$$
$$
\frac{(\frac{1}{\sqrt{\beta_1}} - \frac{1}{\sqrt{\beta_2}})^2 + 1}{(\frac{1}{\sqrt{\beta_1}} + \frac{1}{\sqrt{\beta_2}})^2 + 1}), \qquad (12)
$$

where $F(\cdot,\cdot;\cdot;\cdot)$ is the hypergeometric function [15, eq. (9.100)], and we have replaced $x + 1$ with x in (10) following the results in [16] and used it in $P_e = \frac{1}{\sqrt{4\pi}} \int_0^\infty F_{AF}(x) \frac{e^{-x}}{\sqrt{x}} dx$ to calculate the BER with [15, eq. (6.621.3)]. From (12), one can obtain the results for Rayleigh fading by letting $\alpha_1 = \alpha_2 = 1$. Also, in the asymptotic case when β_A and β_B are very large due to either small path loss or large transmission power, $P_e \propto \frac{1}{\beta_1^{\alpha_1}\beta_2}$. Thus, P_e changes with β_1 at a rate of α_1 and with β_2 at a rate of 1.

If DF is used, the UAV decodes the information sent by the ground user and then sends the decoded information to the remote station or the other way around if the remote station sends data. In this case, the end-to-end SNR can be shown as

$$\gamma_{DF} = \min\{\gamma_A, \gamma_B\}. \qquad (13)$$

Using (13), the outage probability can be derived as

$$P_o^{DF} = 1 - [1 - F_{\gamma_A}(\gamma_{th})][1 - F_{\gamma_B}(\gamma_{th})], \qquad (14)$$

where $F_{\gamma_A}(x) = P(\alpha_1, \frac{x}{\beta_1})$, $F_{\gamma_B}(x) = P(\alpha_2, \frac{x}{\beta_2})$, and $P(\cdot,\cdot)$ is the incomplete Gamma function [15, eq. (8.350.1)]. The BER for BPSK can be derived by averaging the instantaneous BER over the joint probability density function of γ_A and γ_B as

$$P_e^{DF} = H(\beta_1, \alpha_1) + H(\beta_2, \alpha_2) - 2H(\beta_1, \alpha_1)H(\beta_2, \alpha_2), \qquad (15)$$

where $H(x,y) = \frac{1}{2} - \frac{1}{2}\sqrt{\frac{x}{1+x}} \sum_{k=0}^{y-1} \frac{\binom{2k}{k}}{[4(1+x)]^k}$.

Our goal is to find the optimum altitude h that minimizes the total power loss of $Q_A + Q_B$, the overall outage of P_o^{AF} or P_o^{DF}, and the overall BER of P_e^{AF} or P_e^{DF} for maximum reliability using numerical search.

IV. NUMERICAL RESULTS AND DISCUSSION

In this section, numerical examples are given to find the optimum altitude by numerical search. The figures are plotted using the expressions in (5), (6), (11), (12), (14) and (15) for the values of h from 10 m to 3000 m with a step size of 10 m.
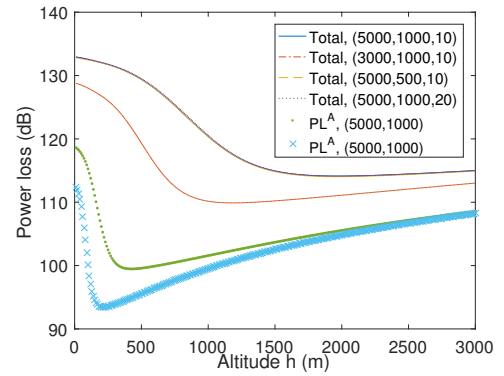

Fig. 2. The total power loss vs. the altitude h for static UAV.

In the examples, we set $f = 2GHz$, $c = 3 \times 10^8 m/s$, $\Omega_A = \Omega_B = 25mW$, and $2\sigma^2 = -100dBm$. Also, we consider the suburban environment where $\eta_{LOS1} = \eta_{LOS2} = 0.1dB$, $\eta_{NLOS1} = \eta_{NLOS2} = 21dB$, $a_1 = a_2 = 5.0188$ and $b_1 = b_2 = 0.3511$ [5]. Note that, since α_U is a function of time t in the mobile UAV case, the power loss, the outage and the BER derived in the previous section are also functions of t for mobile UAV. Consequently, the optimum altitude becomes a function of t for mobile UAV. This is not realistic, as the UAV has to fly up and down consuming more energy. To avoid this, one must average (7), (11), (12), (14) and (15) over the time t. Our study shows that the time-averaged performance of the mobile UAV is almost the same as the static UAV when r_U is less than 1000 meters. Thus, in the following, we only present results for the static UAV, unless otherwise specified.

Fig. 2 compares the total power loss when $m_A = m_B = 1$. In the legend, (5000,1000,10) means $d = 5000$ m, $r_A = 1000$ m and $h_B = 10$ m for total power loss, and (5000,1000) means $d = 5000$ m and $r_A = 1000$ for PL^A etc. One sees that the optimum h that minimizes the total power loss is considerably different from that minimizes PL^A only, as in [5] - [11]. For example, the optimum h is around 400 meters for PL^A in (5000,1000), while it is around 2000 meters for the total power. This leads to a significantly different design for UAV communications. For the total power, the optimum h decreases when d decreases but changes little when h_B increases from 10 meters to 20 meters or r_A decreases from 1000 meters to 500 meters. These results are not obvious from the derivation but are useful to choose system parameters.

Fig. 3 compares the overall outage probability in (11) and (14). As expected, the outage for the user-to-UAV hop only, given by $F_{\gamma_A}(\gamma_{th})$, is lower than the overall outage. Again, they have considerably different values of optimum h, implying the usefulness of our results. For the overall outage, DF is better than AF, as it does not amplify the noise at the UAV, and a shorter distance d leads to a lower outage, as the power loss decreases when d decreases. For AF and DF, under the same conditions, their optimum altitudes are close to each other, giving us the flexibility of choosing different relaying protocols at the UAV. Fig. 4 shows the overall BER in (12) and (15) vs. h. Again, the BER for the user-to-UAV hop only, given by $H(\beta_1, \alpha_1)$, is lower than the overall BER and
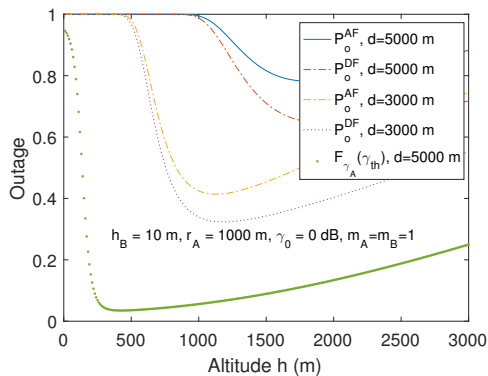
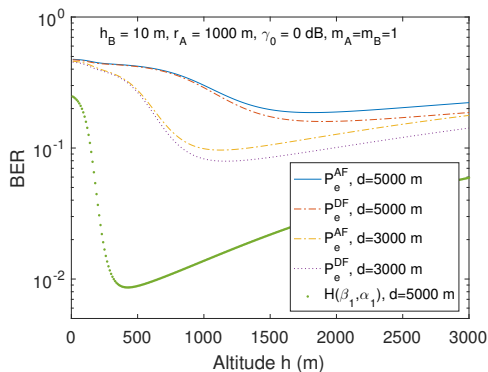Fig. 3.   The overall outage probability vs. the altitude h for static UAV.

Fig. 4.   The overall BER vs. the altitude h for static UAV.

they have considerably different optimum altitudes. DF is still better than AF in terms of BER. It is also interesting to note that for the overall performance under the same conditions, the optimum altitudes that minimize the total power loss, the overall outage and the overall BER are slightly different by comparing Figs. 2 - 4. All these results are useful for UAV communications designs. Fig. 5 shows the BER for different m parameters. The BER performance improves and the optimum altitude increases as the m parameter increases.

V. CONCLUSION

The optimum altitude of UAV as a relay has been studied. The total power loss, the overall outage and the overall BER
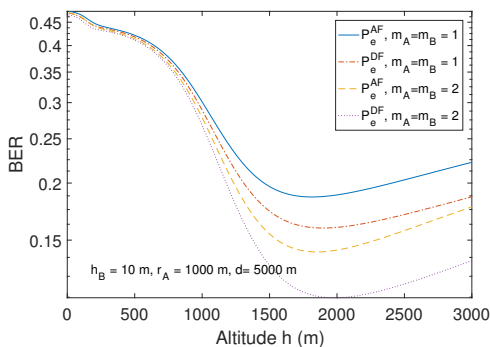

Fig. 5.   BER vs. the altitude h for static UAV with different m parameters.

have been derived and numerically optimized for both AF and DF. Numerical results have shown that different performance measures have slightly different optimum altitudes and that DF performs better than AF. Our study considers a single user at the cell edge. It could be extended to a group of users. In this case, cyclical multiple access can be used [18], [19]. The system-level performance metrics, such as the sum rate or the minimum rate of all users can be maximized. Also, our study does not consider practical factors, such as heading, gyro or acceleration. They can change the distance between transmitter and receiver and hence, affect the performance. However, they are beyond the scope of this letter item.

REFERENCES

[1] S. Hayat, E. Yanmaz, R. Muzaffar, "Survey on Unmanned aerial vehicle networks for civil applications: a communications viewpoint," *IEEE Commun. Surveys and Tutorials*, vol. 18, pp. 2624 - 2661, 4th Q. 2016.
[2] R. Irem Bor-Yaliniz, A. El-Keyi, H. Yanikomeroglu, "Efficient 3-D placement of an aerial base station in next generation cellular networks," *Proc. IEEE ICC 2016*, Kuala Lumpur, Malaysia, May 2016.
[3] M. Mozaffari, W. Saad, M. Bennis, M. Debbah, "Wireless communication using unmanned aerial vehicles (UAVs): optimal transport theory for hover time optimization," *IEEE Trans. Wireless Commun.*, 2017.
[4] Q. Feng, J. McGeehan, E. Tameh, and A. Nix, "Path loss models for air-to-ground radio channels in urban environments," in *Proc. IEEE 63rd VTC-Spring*, May 2006, vol. 6, pp. 29012905.
[5] A. Al-Hourani, S. Kandeepan, S. Lardner, "Optimum LAP altitude for maximum coverage," *IEEE Wireless Commun. Lett.*, vol. 3, pp. 569 - 572, Dec. 2014.
[6] M. Alzenad, A. El-Keyi, F. Lagum, H. Yanikomeroglu, "3D placement of an unmanned aerial vehicle base station (UAV-BS) for energy-efficient maximal coverage," *IEEE Wireless Commun. Lett.*, vol. 6, pp. 434 - 437, Aug. 2017.
[7] M. Mozaffari, W. Saad, M. Bennis, M. Debbah, "Unmanned aerial vehicle with underlaid device-to-device communications: performance and tradeoffs," *IEEE Trans. Wireless Commun.*, vol. 15, pp. 3949 - 3963, June 2016.
[8] M. Mozaffari, W. Saad, M. Bennis, M. Debbah, "Efficient deployment of multiple unmanned aerial vehicles for optimal wireless coverage," *IEEE Commun. Lett.*, vol. 20, pp. 1647 - 1650, Aug. 2016.
[9] J. Lyu, Y. Zeng, R. Zhang, T.J. Lim, "Placement optimization of UAV-mounted mobile base stations," *IEEE Commun. Lett.*, vol. 21, pp. 604 - 607, Mar. 2017.
[10] M.M. Azari, F. Rosas, K.-C. Chen, S. Pollin, "Optimal UAV positioning for terrestrial-aerial communication in presence of fading," *Proc. IEEE GLOBECOM 2016*, Washington DC, USA, Dec. 2016.
[11] V. Sharma, R. Sabatini, S. Ramasamy, "UAVs assisted delay optimization in heterogeneous wireless networks," *IEEE Commun. Lett.*, vol. 20, pp. 2526 - 2529, Dec. 2016.
[12] F. Ono, H. Ochiai, R. Miura, "A wireless relay network based on unmanned aircraft system with rate optimization," *IEEE Trans. Wireless Commun.*, vol. 15, pp. 7699 - 7708, Nov. 2016.
[13] E. Larsen, L. Landmark, O. Kure, "Optimal UAV relay positions in multi-rate networks," *Proc. Wireless Days 2017*, Porto, Portugal, Mar. 2017.
[14] Y. Zeng, R. Zhang, T.J. Lim, "Throughput maximization for UAV-enabled mobile relaying systems," *IEEE Trans. Commun.*, vol. 64, pp. 4983 - 4996, Dec. 2016.
[15] I.S. Gradshteyn and I.M. Ryzhik, *Table of Integrals, Series, and Products*, 6th Ed. New York, NY: Academic Press, 2000.
[16] D. Senaratne and C. Tellambura, "Unified exact performance analysis of two-hop amplify-and-forward relaying in Nakagami fading," *IEEE Trans. Veh. Technol.*, vol. 59, pp. 1529 - 1534, Mar. 2010.
[17] N.C. Beaulieu and Y. Chen, "An accurate approximation to the average error probability of cooperative diversity in Nakagami-m fading," *IEEE Trans. Wireless Commun.*, vol. 9, pp. 2707 - 2711, Sept. 2010.
[18] J. Lyu, Y. Zeng and R. Zhang, "Cyclical multiple access in UAV-aided communications: a throughput-delay tradeoff," *IEEE Wireless Commun. Lett.*, vol. 5, pp. 600 - 603, Dec. 2016.
[19] J. Lyu, Y. Zeng and R. Zhang, "Spectrum sharing and cyclical multiple access in UAV-aided cellular offloading," to appear in *IEEE Globecom 2017*.